Optik 156 (2018) 93–98

Contents lists available at ScienceDirect

Optik

journal homepage: www.elsevier.de/ijleo

Full length article

Characterization of the nanosandwiched Ga_2S_3/In/Ga_2S_3 interfaces as microwave filters and thermally controlled electric switches

S.R. Alharbi[a], Eman O. Nazzal[b], A.F. Qasrawi[b,c,*]

[a] Physics Department, Faculty of Science-Al Faisaliah, King Abdulaziz University, Jeddah, Saudi Arabia
[b] Department of Physics, AAUJ, Jenin, Palestine
[c] Group of Physics, Faculty of Engineering, Atilim University, 06836 Ankara, Turkey

ARTICLE INFO

Article history:
Received 14 August 2017
Received in revised form 29 October 2017
Accepted 30 October 2017

Keywords:
Gallium sulfide
Optical materials
Coating
Microwave resonator
Switches

ABSTRACT

In this work, an indium layer of 50 nm thicknesses is sandwiched between two 500 nm thick Ga_2S_3 layers. The effect of indium nansandwiching on the composition, structure, morphology, light absorbability, capacitance and reactance spectra, and temperature dependent electrical conductivity of the Ga_2S_3 films are investigated by means of X-ray diffraction, scanning electron microscopy, energy dispersion X-ray spectroscopy, Raman spectroscopy, visible light spectrophotometry, impedance spectroscopy and current voltage characteristics. While the nansandwiched films are observed to exhibit an amorphous nature of structure with indium content of Owing to the nucleation mechanisms that take place during the film growth, the accumulation of some unit cells in groups to form grains should be a significant reason for the existence of many different sizes of grains in the nanosandwiched films (Alharbi and Qasrawi, 2016). O, the Raman spectra displayed three vibrational modes at 127.7, 145.0 and 274.3 cm^{-1}. It was also observed that the indium insertion in the structure of the Ga_2S_3 shrinks the energy band gap by 0.18 eV. The nanosandwiched films are observed to exhibit a semiconductor −metal (SM) transition at 310 K. The SM transition is associated with thermal hysteresis that exhibited a maximum value of 16% at 352 K. This behavior of the nanosandwiched films nominate it for use as thermally controlled electric switches. In addition, the impedance spectral analysis in the range of 10–1800 MHz has shown a capacitance tunability of more than 70%. The measurements of the wave trapping property displayed a bandpass/reject filter characteristics above 1.0 GHz which allow using the Ga_2S_3/In/Ga_2S_3 thin films as microwave resonator.

1. Introduction

The Ga_2S_3 compound has recently been widely considered as a result of its technological applicability. It has been employed as optical resonators and second harmonic generators [1]. It can also find it is position as promising smart capacitive switches, Plasmon devices and as wavetraps [2]. The GaAs/Ga_2S_3 interfaces are reported to be suitable for high −power radiation sensing [3]. Owing to its shorter wavelength transparency, the Ga_2S_3 single crystals are also considered as a competitor to pure and doped GaSe in mid-IR and THz applications [4]. Surface morphology, elemental stoichiometry, chemical

* Corresponding author at: Department of Physics, AAUJ, Jenin, Palestine.
E-mail addresses: atefqasrawi@gmail.com, atef.qasrawi@atilim.edu.tr, atef.qasrawi@aauj.edu (A.F. Qasrawi).

https://doi.org/10.1016/j.ijleo.2017.10.177
0030-4026/

states and stability, and crystallinity studies on gallium sulfide which was synthesized by the atomic layer deposition, using hexakis (dimethylamido) digallium and hydrogen sulfide revealed a self-limiting growth process of GaS_x in the temperature range of 125–225 °C [5,6]. Particularly, the growth per cycle is reported to decrease linearly with increasing temperature. The S/Ga ratio exhibited values between 1.0 and 1.2 in the temperature range of 125–200 °C and decreased to 0.75 at 225 °C [5]. It was observed that the growth of these films on single-walled carbon nanotube powders can perform as an excellent electrochemical anode material for use in lithium-ion batteries. Tests on these electrodes have yielded a stable capacity of ≈575 mA/g at a current density of 120 mA/g in the voltage window of 0.01–2.00 V [6].

Early works on the Ga_2S_3 thin films concerned information about the effect of doping processes on the optical performance of this compound. Particularly, it was observed that the Mn doped Ga_2S_3 single crystals prepared by the chemical transport reaction method displayed a dominant emission bands at 1.81 eV and other three weak emission bands at 2.34, 2.14 and 1.54 eV [7]. In our recent works [2,8], we have concentrated on the properties of the Ga_2S_3 in thin film form. The thin films of Ga_2S_3 deposited onto glass and onto Yb, Au and Al metallic thin film substrates were observed to be highly sensitive to the type of substrate. Promising types of plasmonic, metal-semiconductor and metal-semiconductor-metal rectifying devices were fabricated. Here in this work, we aim to report, the results of the nanosandwiching of an indium layer of 50 nm thicknesses between two layers of Ga_2S_3. Particularly, the effects of indium nanosandwiching on the structural, optical and electrical properties of the Ga_2S_3 are studied. The associated thermal hysteresis during the heating and cooling of the samples are reported and discussed. In addition, the alternating current transport dynamics through the sandwiched films is considered in detail.

2. Experimental details

The physical vapor evaporation technique is employed to prepare a 500 nm thick of Ga_2S_3 thin films onto ultrasonically cleaned glass slides from the 99.99% pure Ga_2S_3 powder (Alfa Aeser) under vacuum pressure of 10^{-5} Torr. The resulting fresh films were used as substrates to evaporate 50 nm thin layers of high purity (99.999%) indium. The indium coated Ga_2S_3 films are reused as substrate for the evaporation of another 500 nm thick Ga_2S_3 thin films. The thicknesses of the films were measured with the help of a thickness monitor attached to the system Norm VCM 600 vacuum evaporation system. The nanosandwiched Ga_2S_3/In/Ga_2S_3 films were subjected to X-ray diffraction, scanning electron microscopy, Raman spectroscopy, visible light spectroscopy and impedance spectroscopy analysis using Miniflex 600 diffractometer, Joel JSM 7600 F scanning electron microscope equipped with energy dispersion X-ray (EDX) analyzer, high resolution micro-Raman spectrometer (Thermoscientific DXR), evolution 300 spectrophotometer that is equipped with VEEMAX II reflectometer and 4291 B RF Impedance/Material Analyzer, respectively. The I–V characteristics data were recorded at different temperatures in the range of 300–400 K using a Keithley 230 programmable voltage source and Keithley 6485 picoammeter.

3. Results and discussion

The X-ray diffraction patterns from the top surface of the Ga_2S_3, Ga_2S_3/In and Ga_2S_3/In/Ga_2S_3 interfaces are displayed in Fig. 1(a). The figure illustrates an amorphous structure of the films before and after the sandwiching of indium similar to that of the not sandwiched Ga_2S_3 films [8] indicating that the 50 nm thick indium metal insertion between two 500 nm thick Ga_2S_3 layers does not alter the structure. For the Ga_2S_3/In double layer an intensive peak which is assigned to the tetragonal indium being oriented in the (101) direction is observed (PDF Card No.: 00-005-0642). Coating the indium 50 nm thick layer with 500 nm thick Ga_2S_3 forces this intensive peak to disappear.

To reveal more accurate information about the crystalline nature of the films we have subjected the Ga_2S_3/In/Ga_2S_3 interface to scanning electron microscopy analysis. The image which is shown in Fig. 1(b) represent a 30,000 magnification for the top surface of the films being recorded at an accelerating voltage of 2.0 kV. The image reflects very dense, randomly distribute and spherically shaped particles. Some rarely observed regions exhibit particles of larger sizes. When the image was enlarged 60,000 times (appears in Fig. 1(c)), those particles which are shown in red colored dashed circles exhibit size of ∼ 100 nm. Another group of particles which are also shown in blue dashed circles exhibited size values of ∼ 20 nm. Most of the other remaining particles which are very dark colored in the image of Fig. 1(c) are of 7–10 nm size. Owing to the nucleation mechanisms that take place during the film growth, the accumulation of some unit cells in groups to form grains should be a significant reason for the existence of many different sizes of grains in the nanosandwiched films [8]. On the other hand, when the Ga_2S_3/In/Ga_2S_3 interfaces were subjected to energy dispersion X-ray spectroscopy an elemental atomic contents of 40.7% and 59.3% of Ga and S were detected for the bottom layer. The EDS spectrum of the mapped elements of the Ga_2S_3/In/Ga_2S_3 is illustrated in the inset of Fig. 2(a). For the top layer, the Ga, S and In atomic contents were found to be 41.37% and 56.11% and 2.52%, respectively. Thus, the indium as a doping agent represents only ∼2.52% of the composition. The elemental distribution through the nanosandwich sample as observed from the EDS mapping which are illustrated in Fig. 2. The figure indicate a very dense presence of Ga (Fig. 2(b)) and S (Fig. 2(c)) compared to indium (Fig. 2(d)). The mapping of the indium which is shown in Fig. 2(d) is plotted on blue colored background to allow observation of the indium through the samples. The indium distribution is shown by while color on the blue background.

The Raman spectra for the Ga_2S_3/In/Ga_2S_3 interface are displayed in Fig. 1(d). The spectrum was recorded in the frequency range of 100–3000 cm^{-1}. However, because the spectra did not display any sharp patterns above 300 cm^{-1} it was not shown in the figure. One sharp very intensive peak appears at frequency of 127.7 cm^{-1}. The intensity of this Raman shift is 4650.

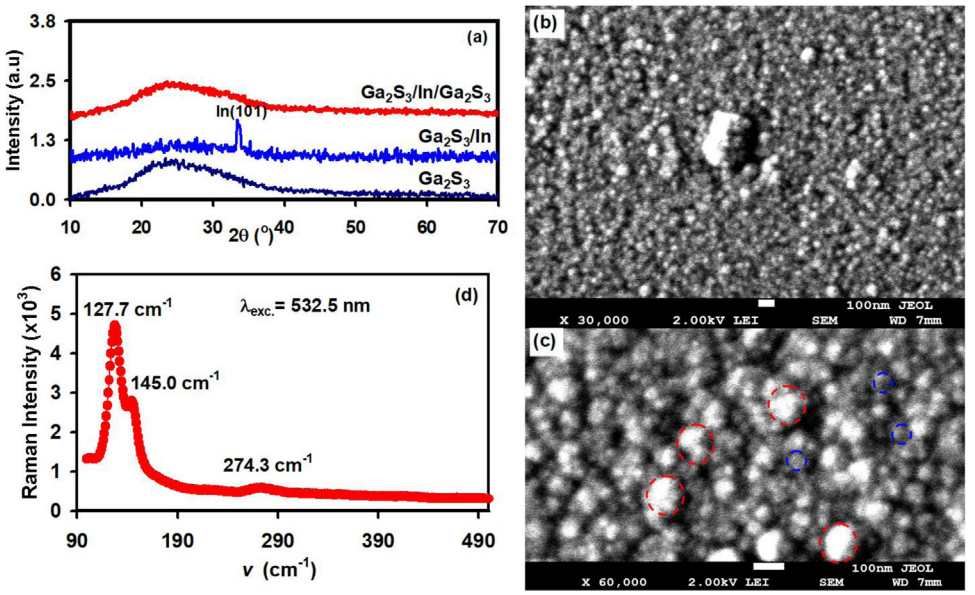

Fig. 1. (a) The X-ray diffraction patterns and the scanning electron microscopy images for a (b) 30,000 and (c) 60,000 magnifications. (d) The Raman spectra for the Ga_2S_3/In/Ga_2S_3 thin films.

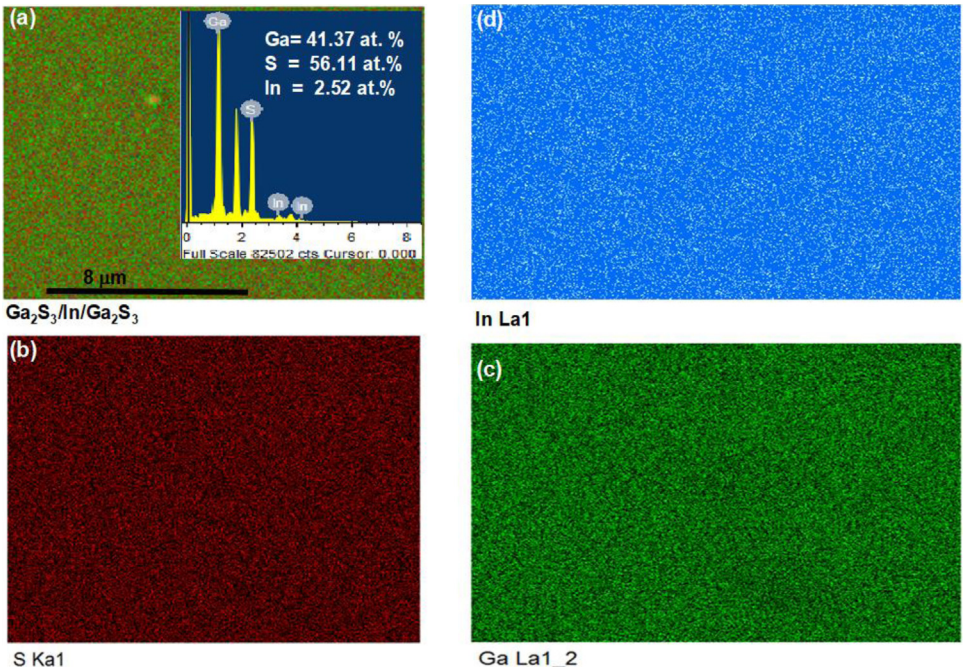

Fig. 2. The elemental mapping of the (a) Ga_2S_3/In/Ga_2S_3, (b) Gallium, (c) sulfur and (d) indium. The inset of (a) show the average EDS results.

This peak exhibits a shoulder at 145 cm^{-1}. Another less sharp peak of intensity of 589 appeared at 274.3 cm^{-1}. The previously observed Raman peaks between 100 and 200 cm^{-1} was assigned to the deformation of the GaS_4 unit in the Ga_2S_3 structure [9]. The shoulder which appeared at 145 cm^{-1} was also observed in the in the Ga_2S_3-Na_2S based glasses at 142 cm^{-1} and was assigned to the charged coupled alkali cation motion which represent the oscillation frequency of the Na ion about its equilibrium position in the potential well defined by the glass former Ga_2S_3. In addition, the Raman shift which is observed at 274.3 cm^{-1} was also observed at 270 cm^{-1} for the Ga_2S_3-Na_2S based glasses in which it showed large dependence on Ga concentration and was assigned to the vibration of S atoms between two edge-shared tetrahedra [9].

In contrast to the expected line shape of Raman spectra, it is also observable from Fig. 1(d) that the Raman peaks are broaden. The intensive peak which is observed at 127.7 cm^{-1} exhibits a full wave half maximum of 19 cm^{-1}. The value

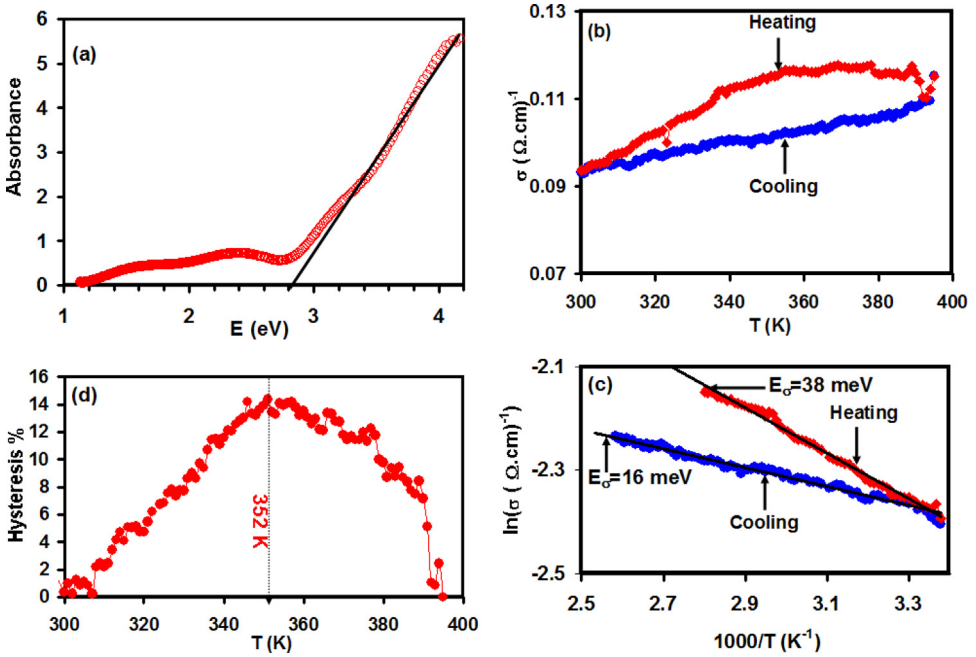

Fig. 3. (a) the absorbance spectra, (b) the temperature dependent conductivity (c) the $\ln(\sigma) - T^{-1}$ variation and (d) the temperature dependent hysteresis percentage for the Ga_2S_3/In/Ga_2S_3 thin films.

confirms the amorphous nature of the films as also observed from the X-ray diffraction and scanning electron microscopy techniques. From Raman spectroscopy point of view, as the medium surrounding a nano-grain never supports the vibrational wavenumbers of a material, phonons are confined within the grain of the nanostructured material. Such confinement significantly alters the vibrational modes in amorphous structures compared to the crystalline ones and results in asymmetric broadening and shift of the optical phonon Raman lines [10]. Particularly, the absence of periodicity beyond the grain dimension leads to relaxation of the zone-centre optical phonon selection rule, causing the Raman spectrum to have contributions also from phonons away from the Brillouin-zone centers [10].

The effect of the indium nanosandwiching on the optical band gap is detected from the absorbance spectra which were calculated from the measured transmittance and reflectance at normal incidence. The spectra that appear in Fig. 3(a) show a linear increase in the values of the absorbance above the absorption edge which is shown by solid line in the same figure. The solid line crosses the energy axis at 2.80 eV. This value of the energy band gap is less than that we have previously reported as 2.98 eV for the pure sandwiched Ga_2S_3 thin films [8]. The shrinkage of the energy band gap via 50 nm indium nanosandwiching could be assigned to the increase in the band tails width. As observed from structural analysis, the indium incorporation into the sandwiched thin films plays role in the lattice distortion and create more disorder in the structure which leads to the optical gap reduction [11]. It is also possible to think that as the ionic radius of indium is larger than that of Ga, the In introduction into the films make the lattice distortion that in turn increases the disorder and give rise to the localized states near the conduction band in the energy band gap of the Ga_2S_3 films [12].

To contribution of indium sandwiching between two layers of Ga_2S_3, to the electrical conductivity (σ) was also studied through the measured σ in the temperature range of 300–400 K. The temperature dependent conductivity is illustrated in Fig. 3(b). Interesting features of electrical conduction is observed upon heating and cooling of the samples. Particularly, during the heating process, the conductivity steadily increases with increasing temperature up to ~380 K where it show a slight decrease in values. During the cooling process, the electrical conductivity follows another slope of variation. It returns to its original value before heating at ~310 K. As presented in Fig. 3(c), in accordance with the equation, $\sigma \propto e^{-\frac{E_\sigma}{kT}}$, the thermal excitation effect on the electrical conductivity is recognized from the values of the activation energies being 38 meV during the heating process and being 16 meV during the cooling process. The room temperature values of the electrical conductivity before and after the nanosandwiching of indium are experimentally determined and found to exhibit values of 8.9×10^{-8} and 9.3×10^{-2} $(\Omega cm)^{-1}$. The electrical conductivity before the indium incorporation is the same during the heating and cooling processes. The activation energy in this temperature range is 330 meV. These numerical values suggest a remarkable increase in the electrical conduction properties of the films and confirms that the insertion of indium establishes shallow impurity levels near the conduction band of Ga_2S_3.

In order to evaluate the hysteresis curve which appears upon temperature variation of electrical conductivity (Fig. 3(b)), the hysteresis percentage ($h\% = 100 \times \left(\sigma_{Heating} - \sigma_{cooling}\right) / \sigma_{Heating}$) was calculated and plotted in Fig. 3(d). The $h\%$ value of the nanosandwiched films increases with increasing temperature up to 352 K where it reaches a maximum value of 16%. Further increase in the temperature decreases the hysteresis percentage to ~1% value at 392 K. Such type of behavior usually appears

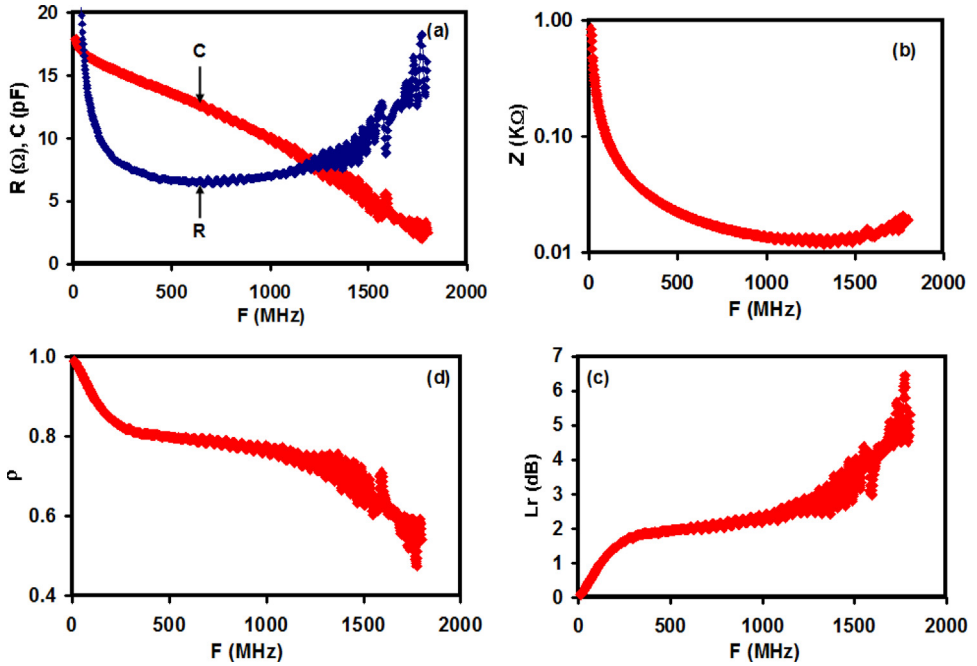

Fig. 4. (a) The resistance, capacitance, (b) impedance and (c) reflection coefficient spectra for the Ga_2S_3/In/Ga_2S_3 thin films.

in materials which exhibit semiconductor – metal (SM) transitions [13]. The semiconductor – metal transition temperature (SMT) in our samples is 310 K. The broad hysteresis and small amplitude of electrical conductivity change is reported to result from the presence of high density of grain boundaries, as appears from the SEM images of Fig. 1(b) and (c), and grain boundary defects [13]. The metallic nature of the films appears during the heating cycle above 352 K, where the conductivity slightly decreases with increasing temperature. Although the SMT is 310 K, the conductivity continues the increasing trend with increasing temperature which a character of persistence of a semiconducting-like behavior and usually happens due to competing contribution of the residual semiconducting phase that causes a positive coefficient of conductivity above the SMT [13].

It is also possible to think that, because the activation energy which can be regarded as an impurity level created by indium atoms during the heating process is deeper (38 meV) than during the cooling process (16 meV), then the SM transition happens as a result of excitation of electrons from 38 meV level to the conduction band minimum and returning to another impurity level (16 me3 V). Consistently, it is possible to believe that the merging of impurity levels to the conduction band minimum upon transition cannot persist beyond the critical concentration [14].

Such type of electrical conduction mechanisms finds application as thermally activated switches. Because it should be possible to stabilize the nanosandwiched films any conductivity value temperature within the hysteresis curve by adjusting the sample's temperature. These switches are run via short heating and cooling pulses. However, further effort must be spent to improve the difference between the "on" (high conductivity) and "off" (low conductivity) state of the Ga_2S_3/In/Ga_2S_3 film as thermally controlled electrical switches to establish a bit higher MST temperature as it is very near to room temperature in its present form.

Another application of the indium nanosandwiched Ga_2S_3 films can be detected from the impedance spectroscopy analysis in the frequency range of 10–1800 MHz. The resistance and capacitance spectra which were recorded at room temperature are displayed in Fig. 4(a). A sharp fall in the resistance and capacitance values are observable upon frequency increase. The decay in the resistance values are much faster than those of the capacitance. The resistance spectra tend to remain constant in the frequency range of 360–1050 MHz. For larger applied frequencies, the resistance (R) starts responding to the applied frequency. On the other hand, the capacitance (C) continually decreased with increasing frequency. It started from a value of 18 pF at 10 MHz and reached a value of 2.5 pF at 1800 MHz. The linear variation of the capacitance with frequency can be presented by the equation, $C(F) = -8.1 \times 10^{-3}F + 17.6\,(pF)$. The tunability of the Ga_2S_3/In/Ga_2S_3 films as capacitors aremore that 72%. This large range of variation of the capacitance nominates the nanosandwiched films to be used in high frequency capacitive circuits. The total effects of the capacitance, resistance and inductance are presented by the impedance (Z) spectra which is also presented in Fig. 4(b). The logarithmic plot of the Z – F dependence reveals a power law of $Z = 5.19F^{0.87}\ (k\Omega)$ in the frequency range of 10–1200 MHz. For higher frequency values the impedance is highly influenced by the resistive part and increases with increasing frequency. The quality of the impedance matches between the source (Z_S) and the nanosandwiched sample (Z_L) is usually presented by the magnitude of reflection coefficient ($\rho = (Z_L - Z_S)/(Z_L + Z_S)$). The less the value of ρ, the better the match. While a ρ value of −1 indicates shorts, the +1 values indicate open loads [15,16]. The

calculated $\rho - F$ spectra are presented in Fig. 4(c). One may see a sharp decrease in the reflection coefficient values in the frequency range of 10–300 MHz, followed by slow variation in the range of 300–1200 MHz and a very fast oscillatory decay as the impeded frequency exceeds 1200 MHz. In general, this type of variation suits the wave traps in the band pass mode. It indicates the applicability of this device as band pass/reject filters above 1200 MHz.

4. Conclusions

In this article we have discussed the possibility of improving the performance of the Ga_2S_3 thin films through the doping by the nanosandwiching technique. Particularly, the insertion of a 50 nm thick indium layers between two layers of 500 nm thick Ga_2S_3 thin films have shown an indium doping content of Owing to the nucleation mechanisms that take place during the film growth, the accumulation of some unit cells in groups to form grains should be a significant reason for the existence of many different sizes of grains in the nanosandwiched films [8]. The analysis of the structural, optical and electrical properties of this nanostructured material was carried out. It was observed that, while the morphology state of the Ga_2S_3 was not altered, the films show a thermally controlled electrical switching and bandpass/reject filtering properties. Some further modification are in need to be carried out to improve the signal quality when employed as wave traps and to make the "on/off" states more distinguishable when uses as temperature controlled electric switches.

Acknowledgments

This article was funded by the Deanships of Scientific Research (DSR) at Arab American University, Jenin, Palestine and at King Abdulaziz University, Jeddah. The authors, therefore, acknowledge with thanks DSR for technical and financial support.

References

[1] Zhang Mingjian, Guocong Guo, Huiyi Zeng, Xiaoming Jiang, Yuhang Fan, Binwen Liu, Optical parametric oscillator and second harmonic generator using monoclinic phase Ga_2S_3 crystal, U.S. Patent 9,513,532 (2016).
[2] S.R. Alharbi, A.F. Qasrawi, Effect of ytterbium, gold and aluminum transparent metallic substrates on the performance of the Ga_2S_3 thin film devices, Curr. Appl. Phys. 17 (2017) 835–841.
[3] H.F. Liu, K.K. Ansah Antwi, N.L. Yakovlev, H.R. Tan, L.T. Ong, S.J. Chua, D.Z. Chi, Synthesis and phase evolutions in layered structure of Ga_2S_3 semiconductor thin films on epiready GaAs (111) substrates, ACS Appl. Mater. Interfaces 6 (2014) 3501–3507.
[4] Z. Huang, J.-G. Huang, K.A. Kokh, V.A. Svetlichnyi, A.V. Shabalina, M. Yu Andreev, G.V. Lanskii, Ga_2S_3: Optical properties and perspectives for THz applications. n Infrared, Millimeter, and Terahertz waves (IRMMW-THz), 2015 40th International Conference On, IEEE (2015) 1–2.
[5] X. Meng, J.A. Libera, T.T. Fister, H. Zhou, J.K. Hedlund, P. Fenter, J.W. Elam, Atomic layer deposition of gallium sulfide films using hexakis (dimethylamido) digallium and hydrogen sulfide, Chem. Mater. 26 (2014) 1029–1039.
[6] X. Meng, K. He, D. Su, X. Zhang, Y. Ch. Sun, H. Ren, W. Wang, L. Weng, Ch. P. Canlas, J.W. Elam, Gallium sulfide-single-walled carbon nanotube composites: high-performance anodes for lithium-ion batteries, Adv. Funct. Mater. 24 (2014) 5435–5442.
[7] J.S. Lee, Young-Hee Won, Hyun-Nam Kim, Chang-Dae Kim, Wha-Tek Kim, Photoluminescence of Ga_2S_3 and Ga_2S_3: Mn single crystals, Solid State Commun. 97 (1996) 1101–1104.
[8] S.R. Alharbi, A.F. Qasrawi, Dielectric dispersion in Ga_2S_3 thin films, Plasmonics 12 (2016) 1–5.
[9] S. Barnier, M. Guittard, M. Palazzi, M. Massot, C. Julien, Raman and infrared studies of the structure of gallium sulphide based glasses, Mater. Sci. Eng. B 14 (1992) 413–417, Based The peak at 90 cm^{-1} is a result of the mode.
[10] A.K. Arora, M. Rajalakshmi, T.R. Ravindran, V. Sivasubramanian, Raman spectroscopy of optical phonon confinement nanostructured materials, J. Raman. Spectrosc 38 (2007) 604–617.
[11] S.B. Ameur, A. Barhoumi, R. Mimouni, M. Amlouk, H. Guermazi, Low-temperature growth and physical investigations of undoped and (In, Co) doped ZnO thin films sprayed on PEI flexible substrate, Superlattices Microstruct. 84 (2015) 99–112.
[12] C.S. Prajapati, P.P. Sahay, Influence of In doping on the structural, optical and acetone sensing properties of ZnO nanoparticulate thin films, Mater. Sci. Semicond. Process. 16 (2013) 200–210.
[13] S. Kumar, Francis Maury, Naoufal Bahlawane, Electrical switching in semiconductor-metal self-assembled VO_2 disordered metamaterial coatings, Sci. Rep. 6 (2016) 37699.
[14] A. Reuben, Dinesh Varshney, K. Jayakumar, Effect of confining potential on the diamagnetic susceptibility of a donor in a spherical quantum dot, J. Comput. Theor. Nanosci. 8 (2011) 189–193.
[15] B.V. Zeghbroeck, Principles of Semiconductor Devices, Univ. Press, Colarado, USA, 2004.
[16] S.E. Al Garni, Atef F. Qasrawi, Impedance spectroscopic analysis of the InSe/ZnSe/InSe interface, IEEE Trans. Electron. Devices 64 (2017) 244–249.